"In presenting the dissertation as a partial fulfillment of the requirements for an advanced degree from the Georgia Institute of Technology, I agree that the Library of the Institution shall make it available for inspection and circulation in accordance with its regulations governing materials of this type. I agree that permission to copy from, or to publish from, this dissertation may be granted by the professor under whose direction it was written, or, in his absence, by the Dean of the Graduate Division, when such copying or publication is solely for scholarly purposes and does not involve potential financial gain. It is understood that any copying from, or publication of, this dissertation which involves potential financial gain will not be allowed without written permission.

[redacted]

ROBERT DAVID WILROY

AN INVESTIGATION OF THE CRITICAL DEPTH IN AN OPEN CHANNEL WITH A NON-RECTANGULAR CROSS SECTION

A THESIS

Presented to

the Faculty of the Graduate Division

by

Robert David Wilroy

In Partial Fulfillment

of the Requirements for the Degree

Master of Science in Civil Engineering

Georgia Institute of Technology

September 1953

AN INVESTIGATION OF THE CRITICAL DEPTH

IN AN OPEN CHANNEL WITH A NON-

RECTANGULAR CROSS SECTION

Approved:

[redacted]

[redacted]

[redacted]

Date Approved by Chairman: April 14, 1954

ACKNOWLEDGMENTS

The writer acknowledges his indebtedness to Dr. Carstens, the thesis advisor, both for the concept of the study and for helpful suggestions in executing the program; to Mr. H. J. Bates for his help in the construction of the equipment; and to Professors Kindsvater and Metcalfe for their help in preparing the manuscript.

Robert David Wilroy

Atlanta, Georgia
September, 1953

TABLE OF CONTENTS

Page

Preface ii

List of Illustrations iv

Abstract vi

Chapter . . . . .

I. Introduction 1

II. Theoretical Considerations 3

III. Equipment and Instrumentation 7

IV. Procedure 12

V. Discussion of Results 13

VI. Conclusions 32

VII. Recommendations 34

Appendix 35

Glossary of Abbreviations 36

Equations Used 37

Bibliography 39

LIST OF ILLUSTRATIONS

Figure		Page
1.	Cross Section of Triangular Channel.	3
2.	Wooden Flume Used in the Investigation	8
3.	Manometers Used in the Investigation	10
4.	Water Surface Profile of Run No. 1	14
5.	Water Surface Profile of Run No. 3	15
6.	Water Surface Profile of Run No. 4	16
7.	Dimensionless Pressure Plus Momentum Diagram for Run No. 1.	18
8.	Dimensionless Pressure Plus Momentum Diagram for Run No. 3.	19
9.	Dimensionless Pressure Plus Momentum Diagram for Run No. 4.	20
10.	Evaluation of the Pressure Plus Momentum Equation in Longitudinal Strips Between the Upstream and Downstream Sections for Run No. 3.	22
11.	Evaluation of the Pressure Plus Momentum Equation in Longitudinal Strips Between the Upstream and Downstream Sections for Run No. 4.	23
12.	Evaluation of the Pressure Plus Momentum Equation in Longitudinal Strips Between the Upstream and Downstream Sections for Run No. 1.	24
13.	Variation in the Ratio of the Celerity of a Small Gravity Wave to the Upstream Velocity in the Longitudinal Strips Across the Channel	26
14.	Variation of Upstream and Downstream Unit Rates of Flow Across the Channel for Run No. 1.	29
15.	Variation of Upstream and Downstream Unit Rates of Flow Across the Channel for Run No. 3.	30

Figure Page

16. Variation of Upstream and Downstream Unit Rates of Flow Across the Channel for Run No. 4. 30

17. Variation of the Froude Number With the Variation of the Depth Across the Channel Upstream 31

18. Actual Cross Section of the Channel Used in the Investigation 37

ABSTRACT

A detailed study of the transition from rapid to tranquil flow was performed in a channel which was nonrectangular in cross section. The sidewalls were vertical and the bottom was sloping (three horizontal to one vertical) in the cross section. Because of the varying depths across the channel, several questions concerning the transition are presented. Firstly, since wave celerity is a function of depth, is a stationary wave front which is perpendicular to the channel axis possible? Secondly, since the Froude number is used as the criterion to distinguish between rapid and tranquil flow, are the varying values of the Froude number across the channel indicative that rapid and tranquil flow can simultaneously exist in the same cross section? Thirdly, since the local Froude number varies across the section, can the Froude number based upon the bulk section be utilized in defining the flow regime?

The results of the study indicated that a stationary wave front which was perpendicular to the channel axis was possible provided the top width is not a function of depth. Velocity and depth traverses were made both upstream and downstream from these waves. Analysis indicated that momentum was transferred laterally across the channel.

The physical definition of rapid and tranquil flow is merely whether the velocity of flow is greater or less than the celerity of a gravity wave. The existence of the stationary wave indicates that the entire cross section was in the rapid flow regime upstream from the wave.

Thus, the simultaneous existence of tranquil and rapid flow in the same cross section was not possible in the section which was used in the experiments.

The bulk Froude number was computed using the mean velocity and the average depth. Three waves were investigated in detail. Two of the waves were of the nonbreaking type. The bulk Froude number in the upstream section was found to have a value less than one for both of the nonbreaking waves, whereas the accepted value of the bulk Froude number is always greater than one for rapid flow.

CHAPTER I

INTRODUCTION

The theory of the hydraulic jump in rectangular channels was first published by Belanger in 1838. The Miami Conservancy district in 1915 completed studies which indicated that the hydraulic jump was an economical method to dissipate energy and prevent scour below hydraulic structures. Since then several studies have been made on rectangular channels for determination of the sequent depth after the jump and the length of the jump.

The need for information on channels with a cross sectional form other than a rectangle became apparent as more use was made of the hydraulic jump. Studies on a circular section by Mr. Lane and Mr. Kindsvater (1) indicated that pressure-plus-momentum equation could be applied to flow conditions in an irregularly shaped channel. Studies of the hydraulic jump in trapezoidal channels were made, by Mr. C. J. Posey and Mr. P. S. Hsing, (2). The hydraulic jump in a trapezoidal channel was found to be unsteady and had wedge-shaped wings formed on each side. The water surface was not level through the jump. The surface was higher in the up stream portions of the wings. Nomographs for calculation of the critical depth were presented by Mr. W. DeLopp (3) in 1948 using the specific energy approach, while in 1948 Mr. P. Z. Kirpich (4) developed dimensionless curves for the same purpose from B. A. Bakhmeteff's studies.

In the analysis of the hydraulic jump, the critical depth is the dividing line between the rapid and tranquil states of flow. The specific energy equation is recommended by two undergraduate college texts (5 and 6) for finding the critical depth in nonrectangular channels. Solution for the critical depth by the equivalent rectangular cross section using the specific energy equation yields a depth that is different from the first mentioned solution. The pressure plus momentum equation for the full section gives a critical depth that is equal to the equivalent rectangular solution by the specific energy methods, while the pressure plus momentum equation for the equivalent rectangular section gives a third different answer.

The purpose of this thesis was to try to determine what the actual critical depth is in an open channel with a nonrectangular cross section. The problem was approached experimentally in this study by the use of water in a triangularly shaped flume. An attempt was made to obtain a uniform velocity across the channel to simplify the situation. The rate of flow was set as nearly as possible to the critical condition. The condition was analyzed by calculations on the total cross section and on longitudinal strips.

CHAPTER II

THEORETICAL CONSIDERATIONS

Even though the actual conditions would not permit the use of the triangular cross section, the theory will be explained using the triangular cross section for simplicity. Fig. 1 is a diagram of the cross section placed on an x-y coordinate system. The bottom slope of the channel is such that $x = my$.

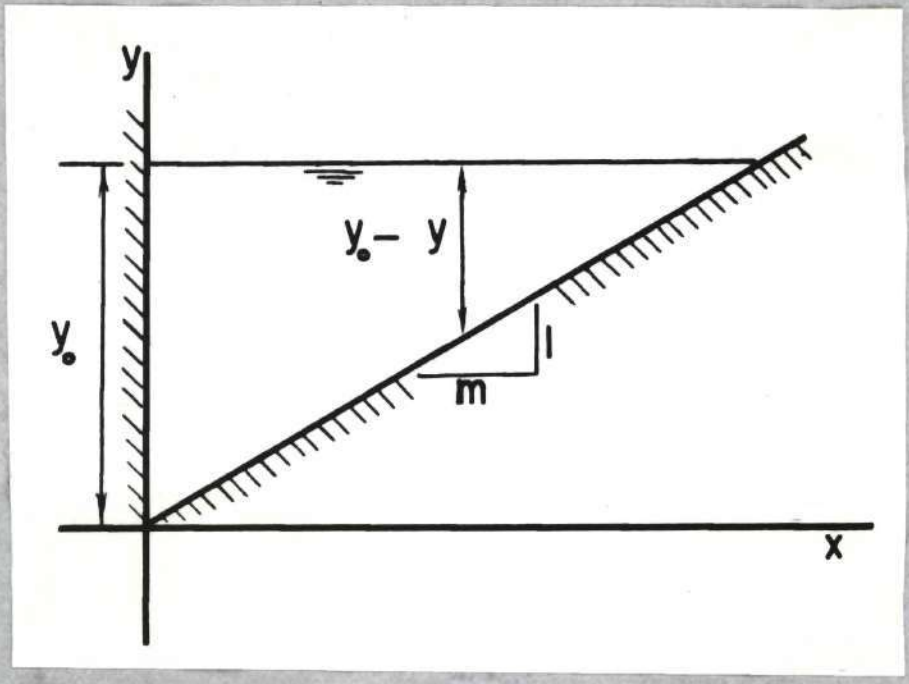

Fig. 1 CROSS SECTION OF TRIANGULAR FLUME

It was assumed that the upstream and downstream cross sections were in zones of essentially hydrostatic pressure distribution. The velocity is also assumed to be uniform over the cross section in this chapter.

The critical depth in an open channel is the depth of flow obtained when the mean velocity is equal to the celerity of a very small gravity wave. In a rectangular channel, the critical depth as defined by the small gravity wave definition is also the point of minimum specific energy on the specific energy versus depth curve. The pressure plus momentum versus depth curve for a rectangular channel gives a depth identical to the critical depth for the point of minimum pressure plus momentum. In a nonrectangular channel, a common value for the critical depth is not obtained as will be shown.

The specific energy approach yields $H_{O_T} = \frac{1}{A}\int_A \left[\frac{v^2}{2g} + (y_o - y)\right] dA$ for the total specific energy across the triangular channel. By differentiating the total specific energy equation with respect to y_o and setting the first derivative equal to zero, the critical depth is found to be $y_{o_c} = \sqrt[5]{\frac{12Q^2}{gm^2}}$ for a constant rate of flow.

The pressure plus momentum approach for the actual triangular cross section gives $\gamma M_o = \rho QV + \frac{\gamma y_o}{3}\frac{(my_o^2)}{2}$ for the total pressure plus momentum. By differentiating this expression and setting the first derivative equal to zero, the minimum point or critical depth is found to be: $y_{o_c} = \sqrt[5]{\frac{8Q^2}{gm^2}}$.

In solution of the equivalent rectangular section using $y_{M_c} = \sqrt[3]{q^2/g}$, where $q = Q/my_{o_c}$ and $y_{M_c} = y_{o_c}/2$, the critical depth is found to be: $y_{o_c} = \sqrt[5]{\frac{8Q^2}{gm^2}}$ which is identical to the critical depth as determined from the pressure plus momentum equation for the actual triangular cross section.

This solution, $y_{o_c} = \sqrt[5]{\frac{8Q^2}{gm^2}}$, is also identical to the solution obtained by the method presented by V. L. Streeter (7) and J. K. Vennard (8) in their texts where the full depth of the channel was used as the static pressure force for the specific energy equation even though the channel was of variable cross section.

The pressure plus momentum equation for the equivalent rectangular section is $\gamma M_o = \rho QV + \gamma \frac{(y_o)}{2} \frac{(my_o^2)}{2}$ which gives a $y_{o_c} = \sqrt[5]{\frac{32Q^2}{3gm}}$. This solution differs from the y_{o_c} of the actual cross section by the difference between the distance from the water surface to the centroid of the rectangle and to the centroid of the triangle. At any time the equivalent rectangle is used, the pressure part of the pressure plus momentum equation should be derived from the original cross section for a correct solution.

In the gravity wave analysis for the critical depth, the ratio of the mean velocity to celerity of a very small gravity wave is equal to the Froude number, $V/\sqrt{gy}$. Therefore, the critical depth in the non-rectangular cross section is the depth at which the Froude number, in which y is the mean depth, y_M, is equal to one (9). By substituting Q/A for the velocity in the Froude number $\sqrt{\ }$ and with $\sqrt{\ }$ equal to one, the critical depth is found to be: $y_{o_c} = \sqrt[5]{\frac{8Q^2}{gm^2}}$.

In the longitudinal strip analysis, the Froude number will vary as the square root of the depth. The Froude number will therefore increase from the deep side of the channel toward the shallow side, and as the depth on the shallow side approaches zero, the Froude number will approach infinity. This is reflected in the ratios of the depth after the jump, y_2, to the depth before the jump, y_1, which for Froude numbers greater than two

is given as $y_2/y_1 = 1/2(\sqrt{1 + 8\ F_1^2} - 1)$. For Froude numbers greater than one but less than two, the ratio of the depths is given by the equation for a finite gravity wave with no breaks in the surface as $y_2/y_1 \approx 4/3(F_1 - 1) + 1$. As the Froude number increases above one, y_2/y_1 also increases. The solution of the above equation for y_2 gives a maximum elevation in the water surface somewhere between the wall on the deep side and the point where the depth is equal to zero on the shallow side. At a mean Froude number close to one, the highest elevation in the water surface profile is approximately one third of the distance from the side where the depth goes to zero. At a mean Froude number of two, the highest elevation in the water surface profile is approximately one third of the distance from the wall on the deep side. This difference in the water surface elevation is an explanation of the observed increase in depth on the upstream wing walls found in the hydraulic jump as observed in a trapezoidal channel. (10) At an upstream depth of 0.01 feet in the cross section, the evaluation of the downstream depth from both equations gives a value varying between 0.05 and 0.10 feet for Froude numbers between 1.0 and 2.0. This large increase in depth is of great importance in this study as it is an explanation of the reverse flow which developed on the shallow side of the full triangular shaped flume. The reverse flow prevented the use of a full triangular cross section.

The longitudinal strip analysis of the Froude number also indicated that it was possible to have a Froude number of less than one in one part of the channel with a Froude number of greater than one in another part of the channel. If this is true, tranquil flow and rapid flow could exist through the same cross section at the same time.

CHAPTER III

EQUIPMENT AND INSTRUMENTATION

All equipment required for this study was available or constructed in the hydraulic laboratory of the Civil Engineering Department of Georgia Tech.

The flume used in this research was 18 feet long and 3 feet wide. The cross section of the flume had a bottom slope of one to three with vertical side walls as shown in Fig. 2. Exterior plywood was used for construction of the flume with a plastic coating being applied for water proofing and obtaining a smooth finish.

The inlet was triangular in shape with the top being horizontal and perpendicular to the deep side. The maximum depth of the inlet opening was 0.40 feet, and the maximum width was 1.20 feet. The forebay side of the opening had one-quarter rounds with a 1-1/2 inch radius connected to the top and bottom. Two vertical walls were placed in the forebay next to the deep and shallow ends of the inlet.

A cover plate, six inches wide, was connected to the downstream side of the inlet to obtain a better velocity distribution. Suction lines for boundary layer control were connected to the cover plate on the shallow side. The suction lines became necessary in this section because of the large amount of surface area in comparison to the flow area.

The unstable condition created by the reverse flow on the shallow side created a necessity for some means of splitting the flow at the inlet.

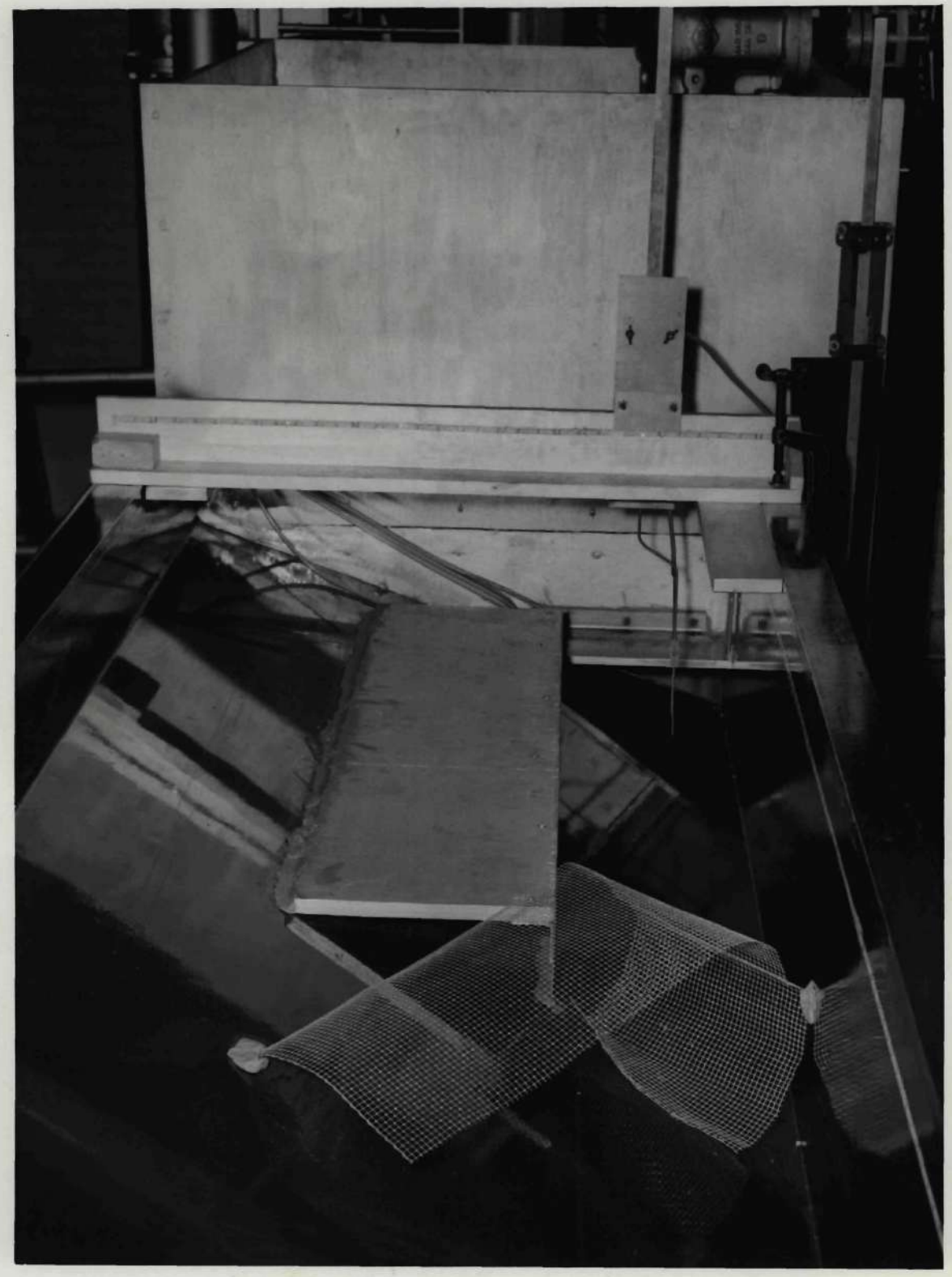

Fig. 2 Wooden Flume Used in the Investigation

A board was installed to separate the main body of flow from a small portion on the shallow side. The board was extended downstream for a distance of three feet where the small portion of the flow was permitted to rejoin the main body.

Adjustment screws were placed under each leg of the flume for use in leveling and placing the flume on a set slope. The first run was made with the flume level, and the downstream end of the flume acted as the control. The last three runs were made on a slope of 0.006, and a piece of fine wire for roughness, as shown in Fig. 2, was used as the control. The fine wire worked very well because only a small amount of energy change was required for control while the average flow was close to the critical flow condition.

Water for the test runs was supplied from the constant head tank in the hydraulic laboratory.

The instruments used in this study with the exception of the point gage, stagnation tube, and transit are shown in Fig. 3. Velocities were determined from stagnation tube measurements. The stagnation tube was connected to one leg of a water-air differential manometer. The other leg of the manometer was connected to a well pot containing a point gage which was preset at the inlet elevation. Two manometers were used to read the deflection for the velocity measurements. A manometer reading to the nearest 0.001 feet was used for Runs No. 1 and 2. The small deflections obtained in Run No. 2 caused high inaccuracies, and the run was discarded. A manometer reading to 0.001 inches was then used for Runs No. 3 and 4.

A point gage mounted on a movable bridge was used to measure the water surface profile. The water surface profile was measured to the

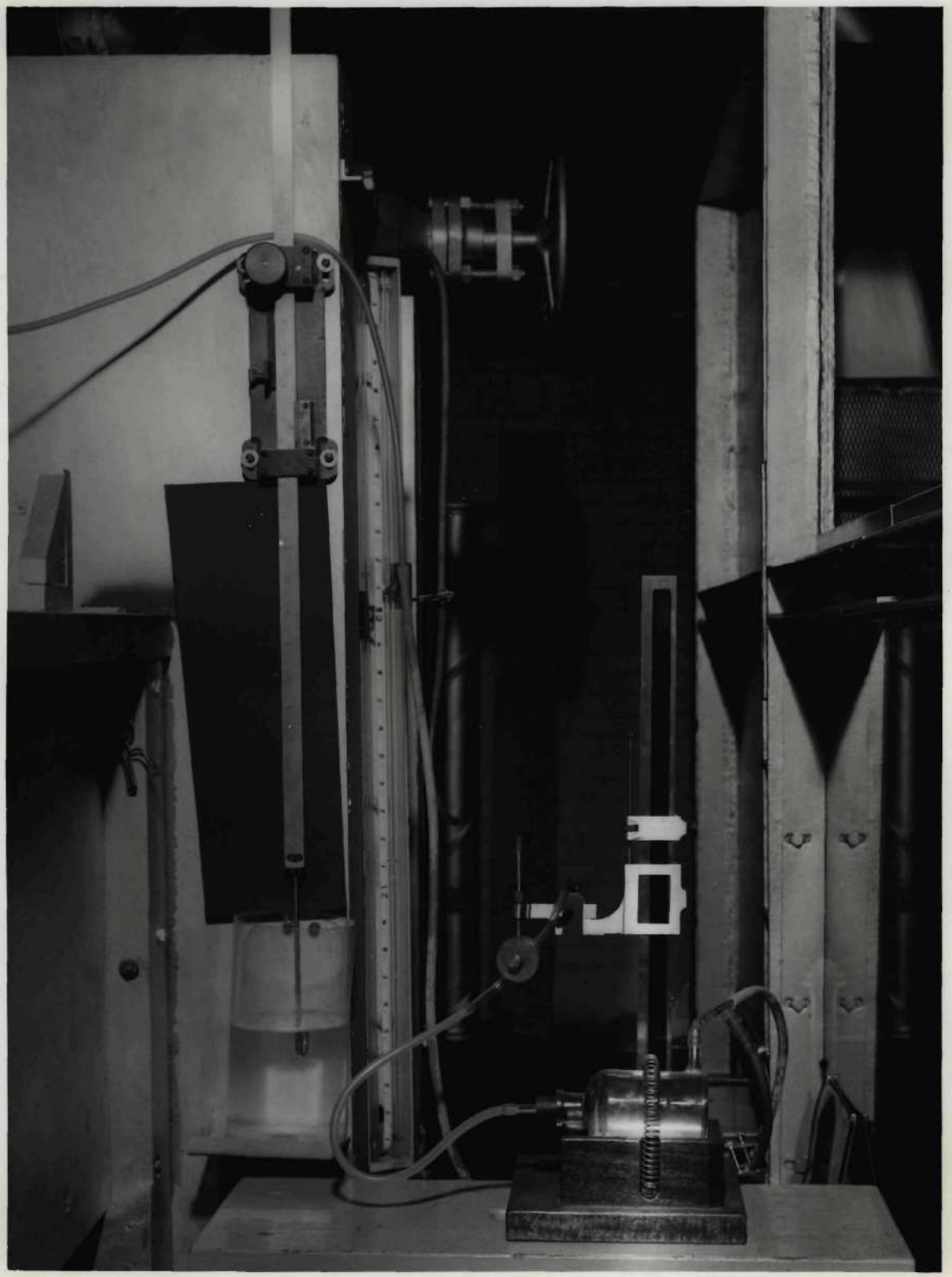

Fig. 3 Manometers Used in the Investigation

nearest 0.001 feet. The flume was leveled with the aid of surveyor's transit reading to the nearest 0.001 feet.

CHAPTER IV

PROCEDURE

The desired rate of water flow in the flume was first established. A wave was then moved into the desired position by the movement of the wire roughness. A water surface profile was then taken. The profile was taken longitudinally with a variation of distance in accordance with the change in the water surface curvature. The profile was taken at preset stations laterally at each longitudinal position.

A velocity traverse was then taken upstream as close to the lip as possible. The same preset stations were used laterally with the vertical distance starting at 0.02 feet from the water surface. Manometer deflections were taken at this position and at every 0.05 feet vertically down until the bottom of the flume was reached. The downstream velocity traverse was taken in the same manner where the water surface was level following the jump for Run No. 1, and at the low point in the surface past the first wave for Run Nos. 2, 3, and 4.

On completion of each run, the profile of the channel floor was recorded in the cross section where the velocity traverses were taken.

The rate of flow was determined by finding the unit rate of flow at each preset station and then integrating the area under a plot of unit rate of flow versus the distance across the channel. The area under all curves was obtained by the trapezoidal rule. The areas used to determine the pressure forces were obtained from the water surface profile.

CHAPTER V

DISCUSSION OF RESULTS

The test runs could be broken down into two general classes. Class I consisted of a well developed jump on the shallow side of the channel and an undulating wave with a well developed roller on the top of the wave located on the deep side of the channel. Class II consisted of an undulating wave completely across the channel with a slight roller on top. The slight roller was unstable on the deep side of the channel. Run No. 1 was of the Class I type, while Runs No. 3 and 4 were of the Class II type. A plot of the water surface profile for each run can be seen in Figs. 4, 5, and 6.

The water surface profile of Run No. 1, as can be seen in Fig. 4, shows that the surface was higher in the deep part of the cross section at the top of the first undulating wave, while the narrow part on the shallow side with the well developed jump had a steady rising surface after the front of the jump. The water surface profiles for Runs No. 3 and 4 show that the water surface was sloped toward the shallow side at the crest of the first wave, and then was sloped toward the deep side at the bottom of the trough following the first wave. This is reasonable from the fact that the part which rises the highest above the normal depth downstream would then go the furthest below the normal depth in the undulating wave before equilibrium is reached downstream. (12) The slope of the water surface at the crest of the first wave in all runs did not

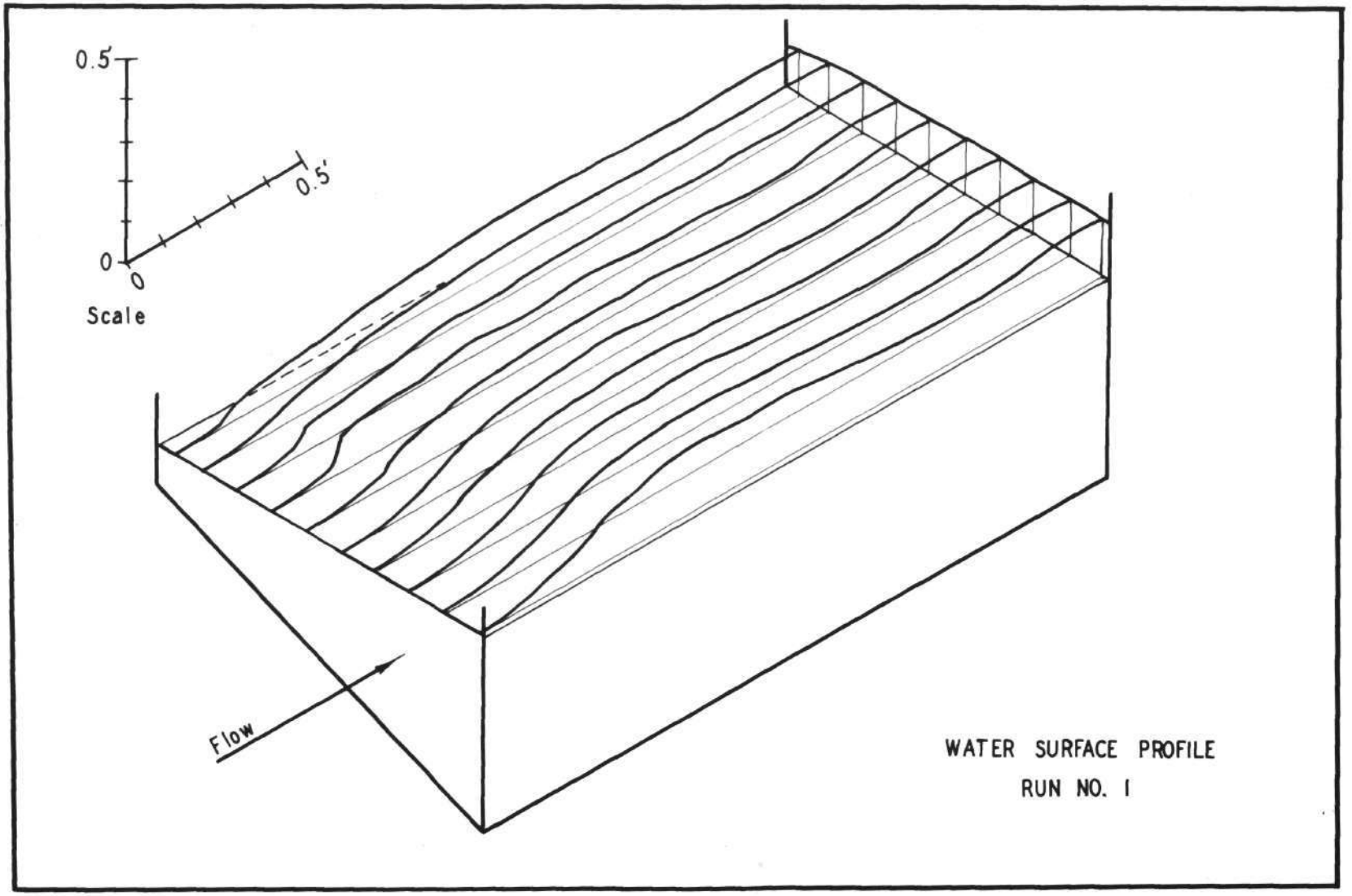

Fig. 4 Water Surface Profile of Run No. 1

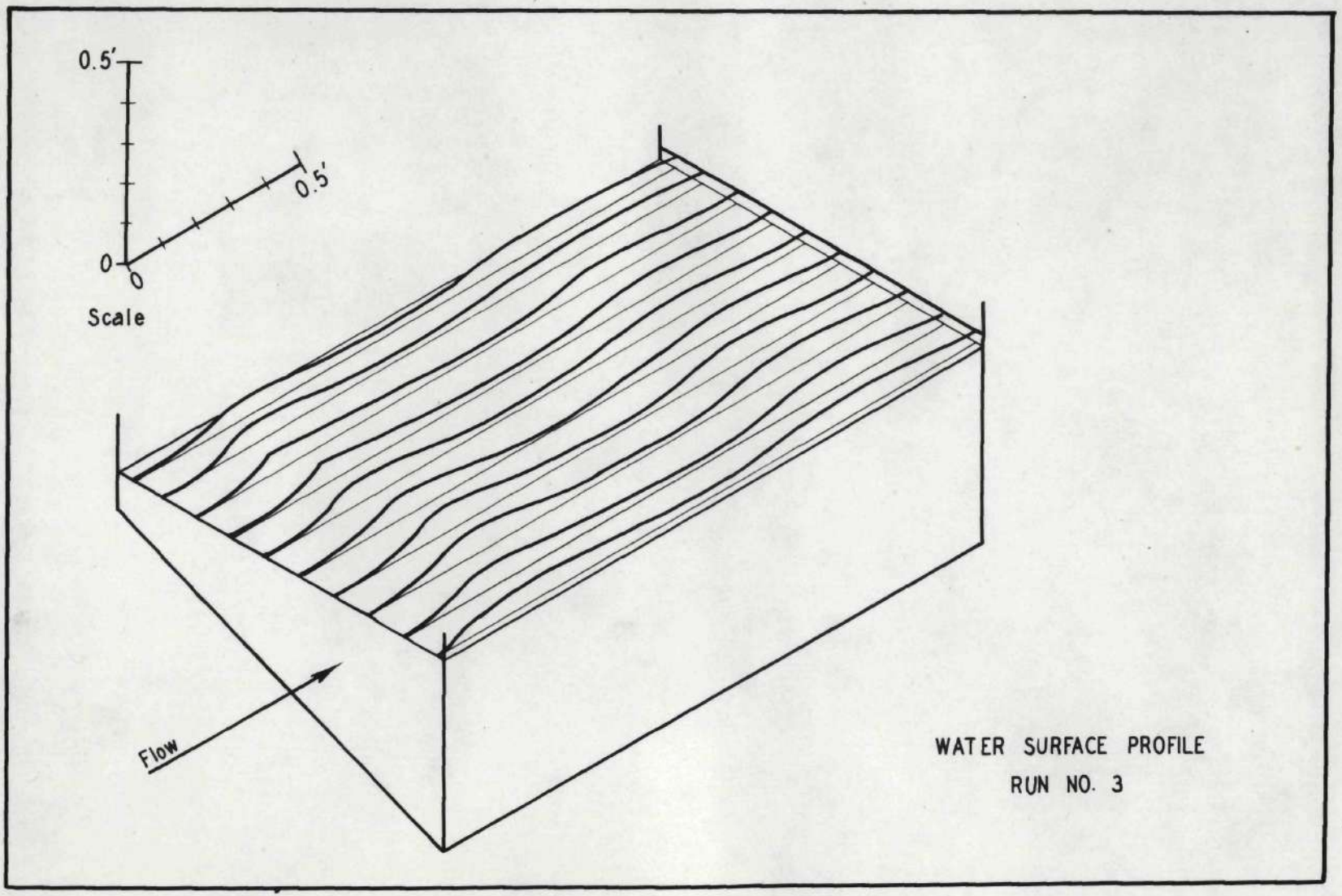

Fig. 5 Water Surface Profile of Run No. 3

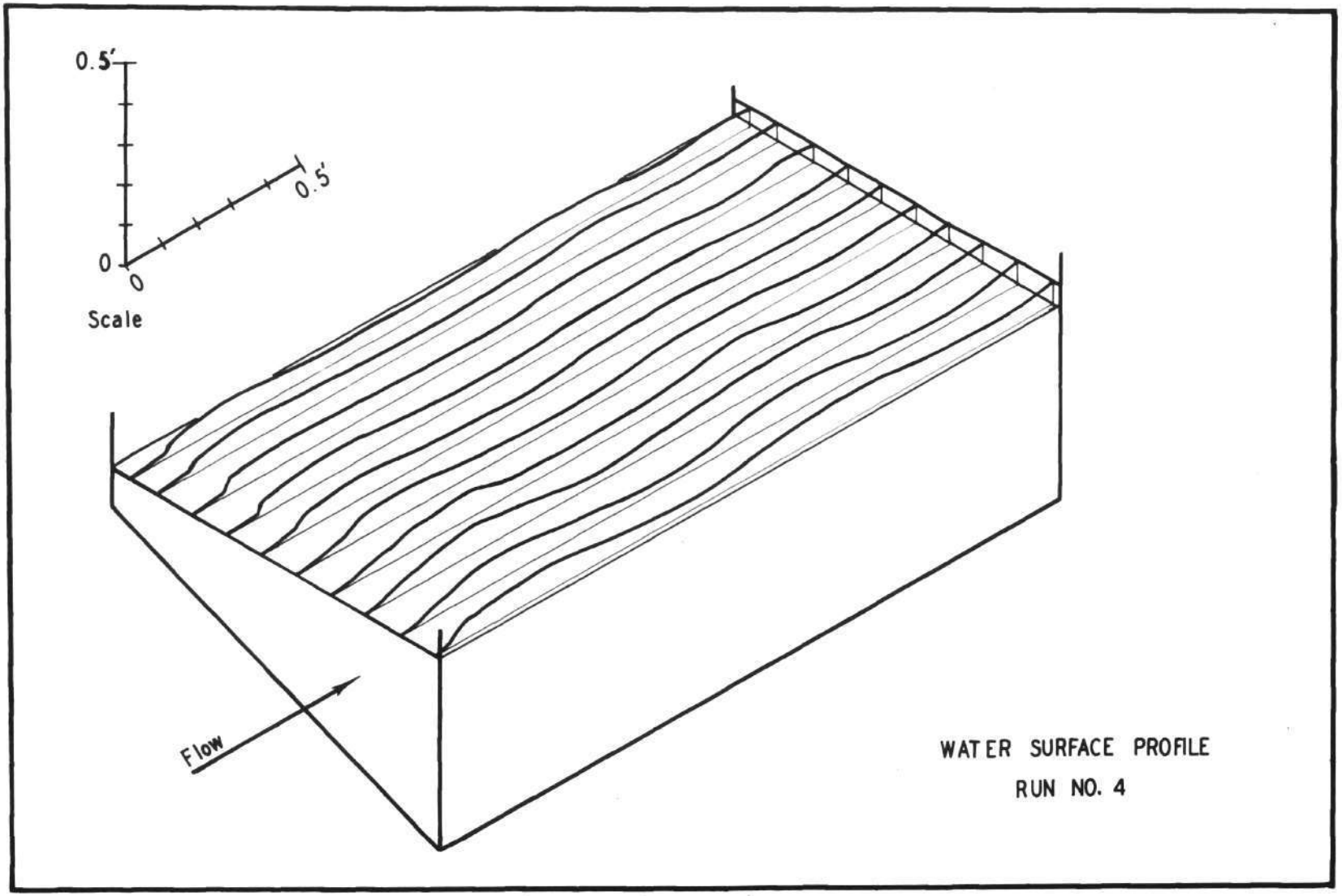

Fig. 6 Water Surface Profile of Run No. 4

agree with the slope of the water surface as calculated from the formulas for finite gravity waves. The reason for the difference will be explained in the discussion of the longitudinal strip analysis.

The pressure plus momentum of the total cross section was plotted against the average depth as shown in Figs. 7, 8, and 9. The plot was made dimensionless by the use of the mean critical depth, y_{M_c}, as defined by A. T. Ippen. (12) Run No. 1 is shown in Fig. 7 to be too far from the critical depth to yield the desired information. Runs No. 3 and 4 are shown in Figs. 8 and 9 to have both the upstream and downstream points above the critical point on the curves. While mathematically this indicates that the average flow in the cross section was in the tranquil state at the inlet, the physical picture of the standing wave shows that the average flow was in a rapid state at the inlet. If the flow had been in a tranquil state, the wave would have moved upstream and submerged the inlet. If the flow upstream was in a rapid state, then the depth upstream must have been less than the true critical depth.

The effect of the momentum correction factor, β, can also be noted in Figs. 7, 8, and 9. The effect of β is to increase the critical depth as β increases. Even though the value of β was small in this study, its effect was noticeable on the location of points on the pressure plus momentum curves. The calculated upstream values for Runs No. 3 and 4 were still within the tranquil range on the pressure plus momentum curves after consideration of the β correction.

The value of the total specific energy for the cross section was determined for Runs No. 3 and 4, using the rate of flow obtained in each

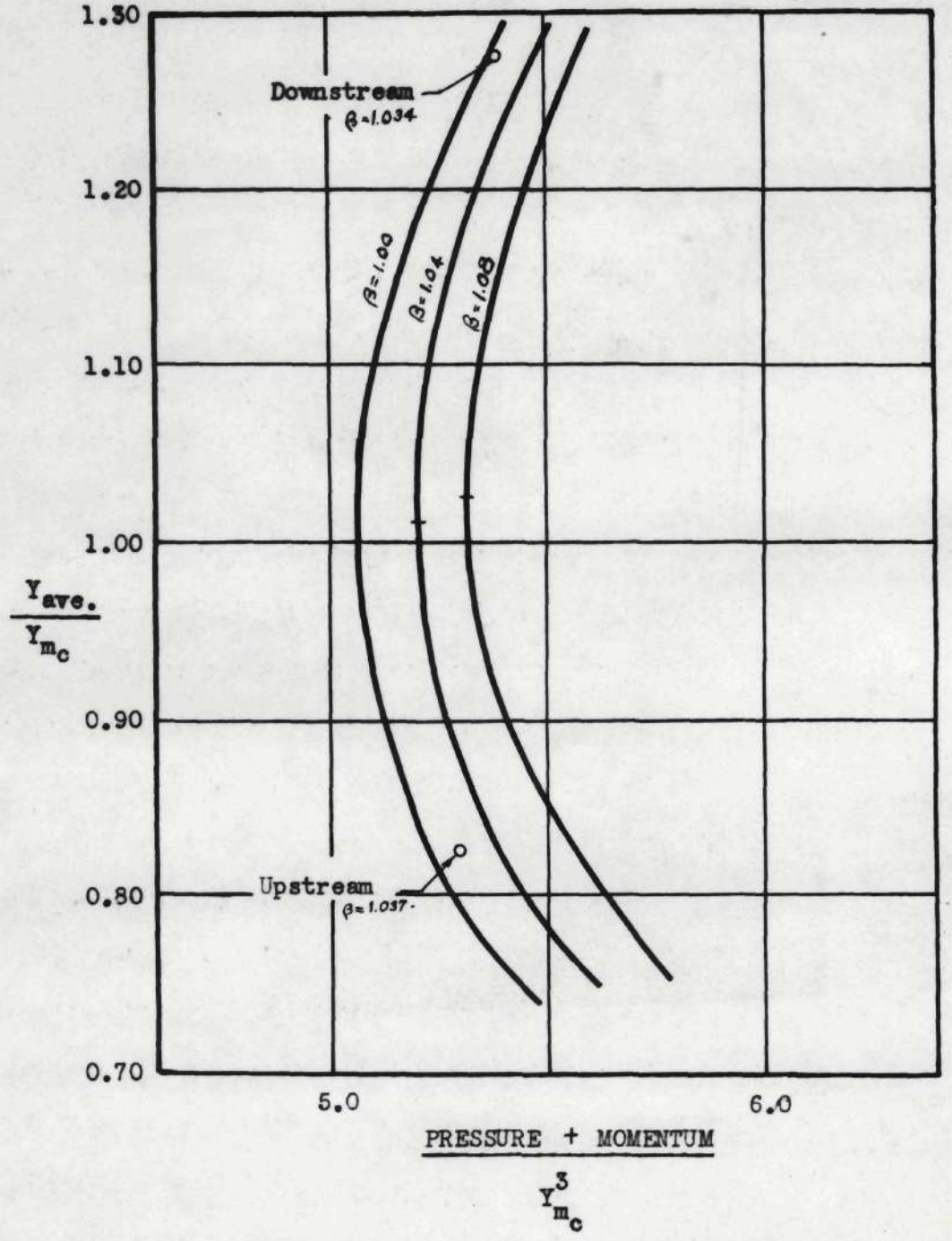

Fig. 7 Dimensionless Pressure Plus Momentum Diagram for Run No. 1

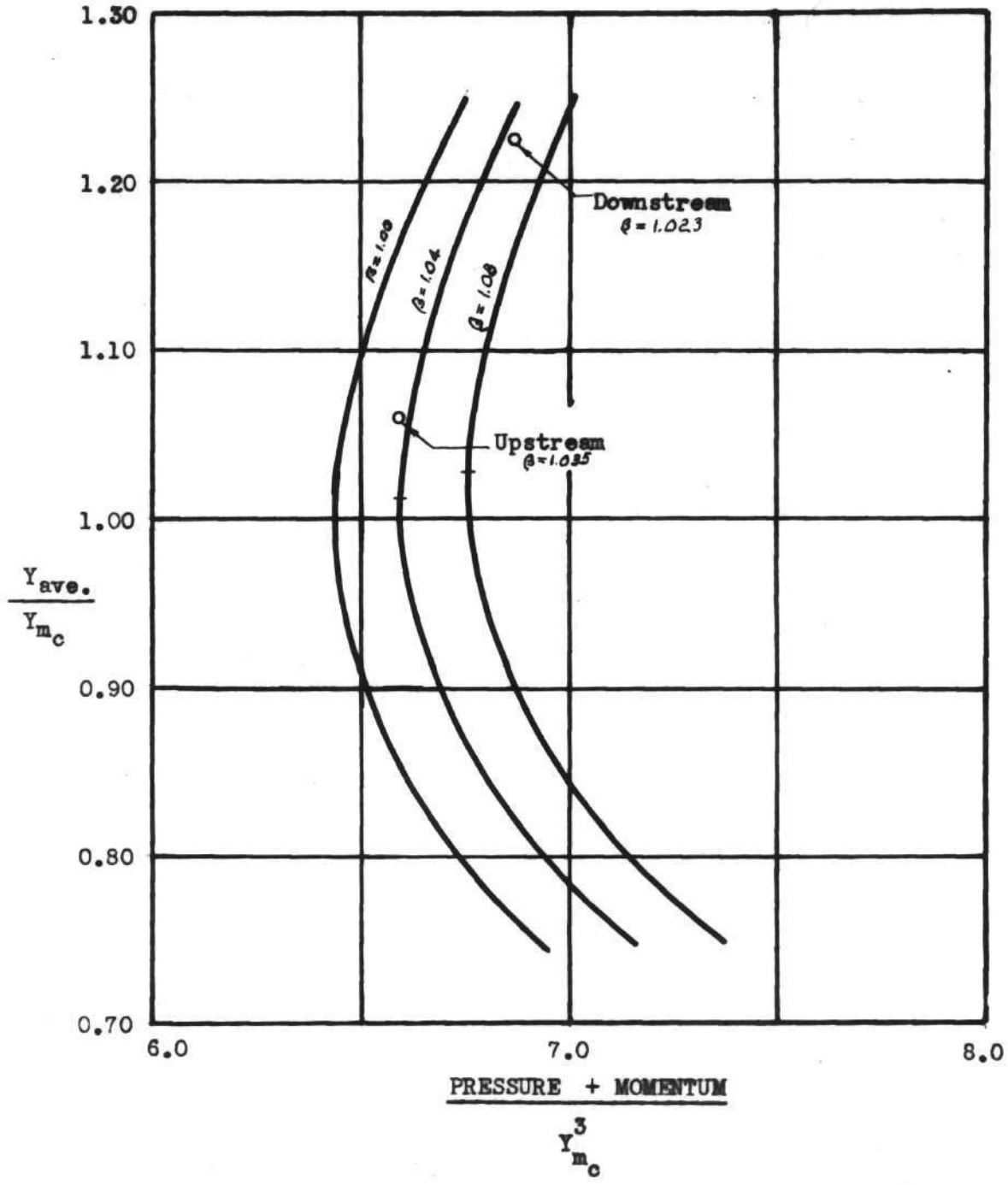

Fig. 8 Dimensionless Pressure Plus Momentum Diagram for Run No. 3

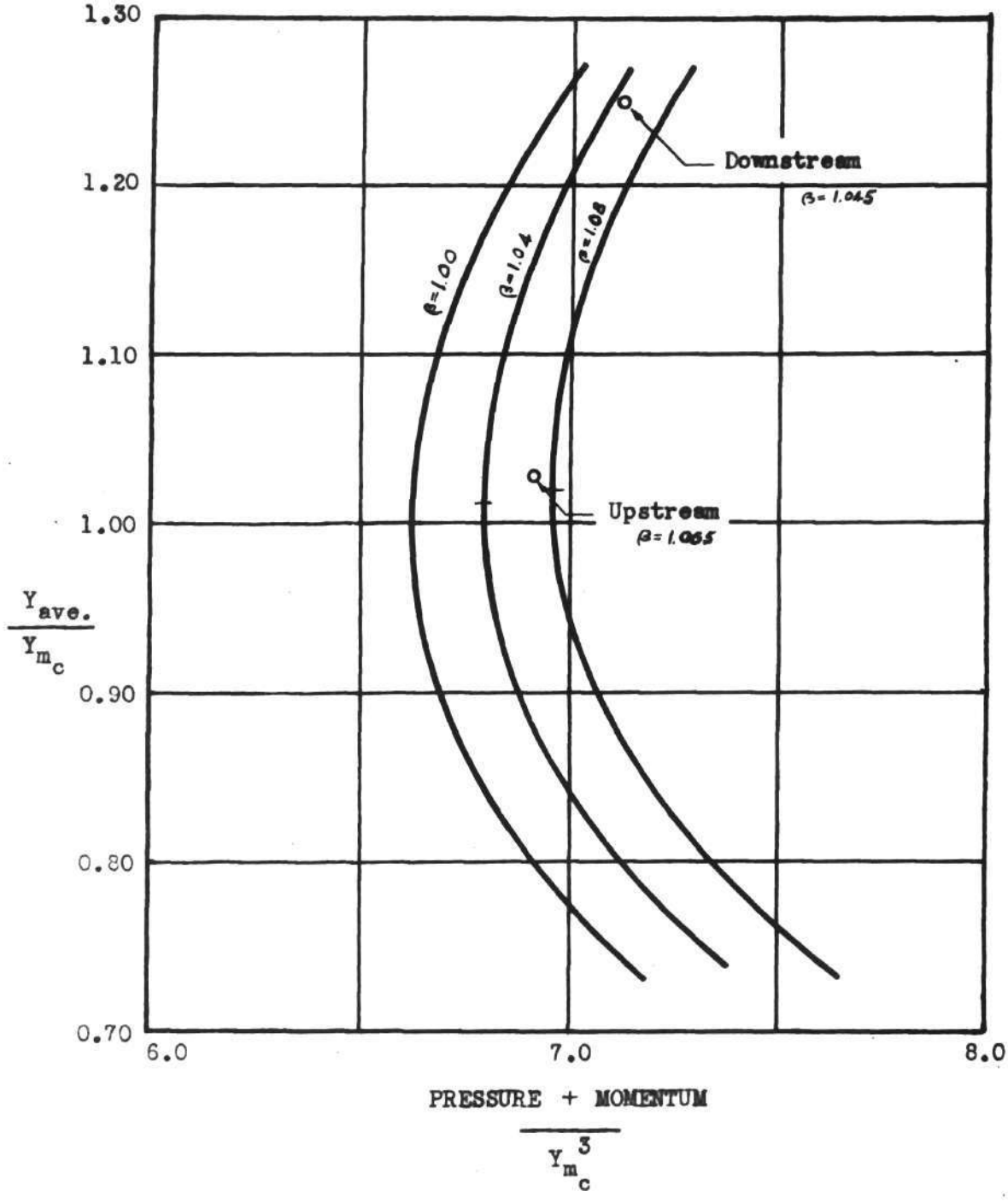

Fig. 9 Dimensionless Pressure Plus Momentum Diagram for Run No. 4

run and different depths. The values of the specific energy were plotted on curves using $y_{ave.}$ for one axis and H_{O_T} as the other axis. The values of the specific energy for the actual cross section were plotted on the two sets of curves. The actual specific energies in the upstream cross sections of Runs No. 3 and 4 were larger than the minimum specific energy and at a greater depth. This would also indicate mathematically that the flow was in a tranquil state upstream, but again the standing wave was present to show that the flow was in a rapid state. The kinetic energy correction factor, α , had the same type of effect on the specific energy equation that β had on the pressure plus momentum equation.

In the longitudinal strip analysis, the pressure plus momentum equation was written between a vertical line in the cross section upstream and a vertical line in the cross section downstream at the same distance from the wall on the deep side. In this analysis, the difference in the momentum forces was divided by the difference in the pressure forces. If the result of the calculation was equal to one, then there was no movement of momentum into or out of the strip between the upstream and downstream points. If the result was greater than one, there was a movement of momentum out of the strip between stations, and a momentum deficiency was created downstream. If the result was less than one, a momentum surplus was created downstream. In the actual calculations, the result was not equal to one in any case. This is readily seen in Figs. 10, 11, and 12. The deficiency in Figs. 10 and 11 is greater than the surplus by the amount of the fluid weight component which was neglected in this calculation. Figs. 10 and 11 show a transfer of momentum from the deep side to the shallow side of the channel.

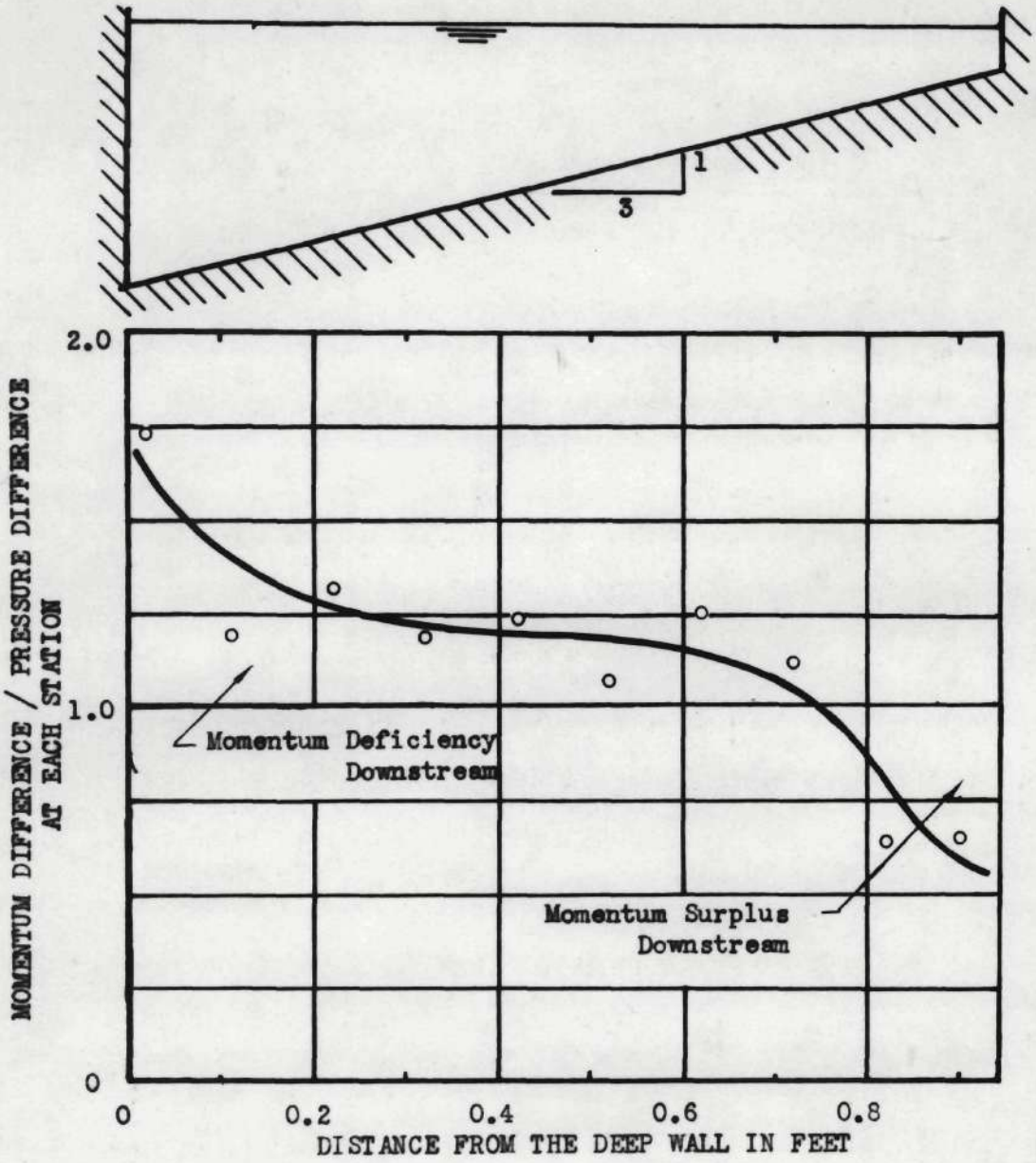

Fig. 10 Evaluation of the Pressure Plus Momentum Equation in Longitudinal Strips Between the Upstream and Downstream Sections for Run No. 3

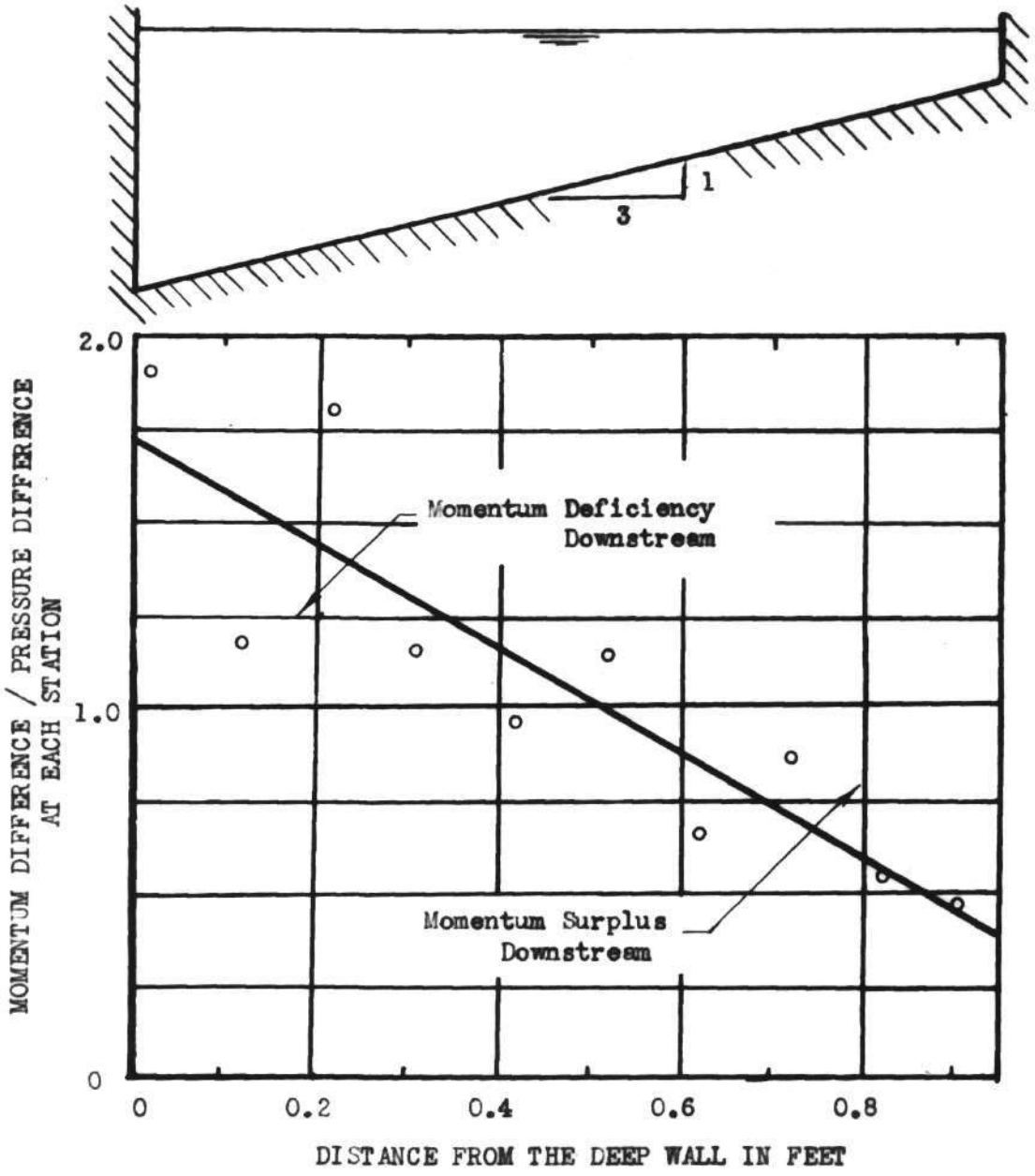

Fig. 11 Evaluation of the Pressure Plus Momentum Equation in Longitudinal Strips Between the Upstream and Downstream Sections for Run No. 4

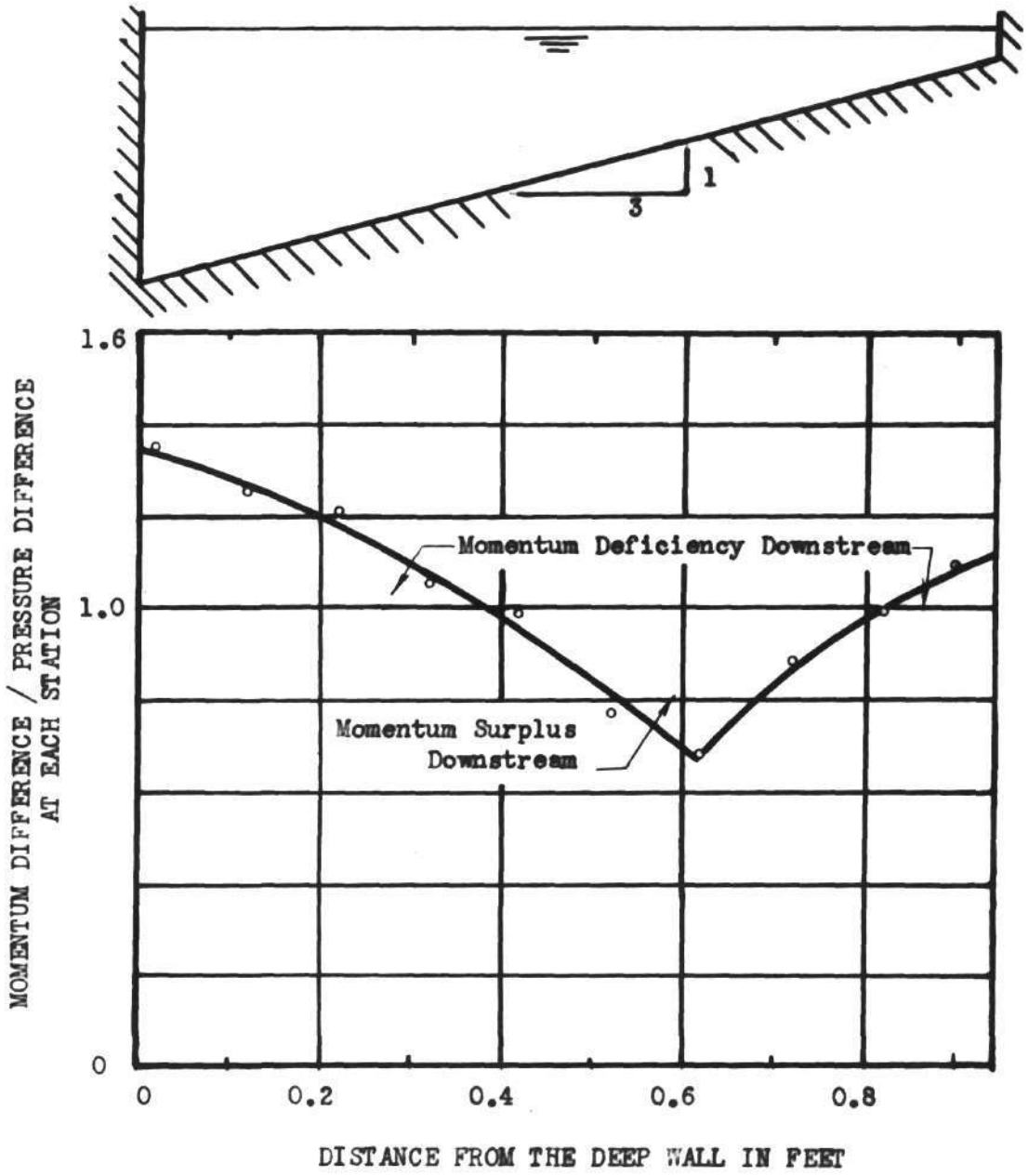

Fig. 12 Evaluation of the Pressure Plus Momentum Equation in Longitudinal Strips Between the Upstream and Downstream Sections for Run No. 1

In Run No. 1, as shown in Fig. 12 there is a transfer of momentum from the shallow side as well as from the deep side. The hydraulic jump on the shallow side in Run No. 1 was well developed. This was completely different from the water surface profile obtained in the other part of the cross section. The profile in the deep section of the channel was comparable to the profile of Runs No. 3 and 4. The inclined water surface across the front did not extend all of the way across the channel as can be seen in Fig. 4. The water surface was level on the shallow side of the channel.

The momentum transfer is a movement of momentum along the wave front. Even though the wave front was approximately perpendicular to the direction of flow, the front was tending to be further upstream on the deep side and further downstream on the shallow side for Runs No. 3 and 4. This tendency can be expressed in the ratio of the celerity of the gravity wave calculated from the actual depths to the velocity in the upstream longitudinal strip. If the ratio of the wave celerity to the upstream velocity, c/v_1, is greater than one, the wave would be tending to move upstream. If c/v_1 is less than one, the tendency is for the wave to move downstream. In Runs No. 3 and 4, the ratio of the wave velocity to the upstream velocity in each strip was in all cases greater than one, but there was a constant decrease in the value of the ratio from the deep side of the channel toward the shallow side as can be seen in Fig. 13. Therefore, the wave front was trying to move upstream at all points in the cross section, but with a front that was tending to be further upstream on the deep side and tending to slope downstream across the channel toward the shallow side. The transfer of momentum along the front, as seen in

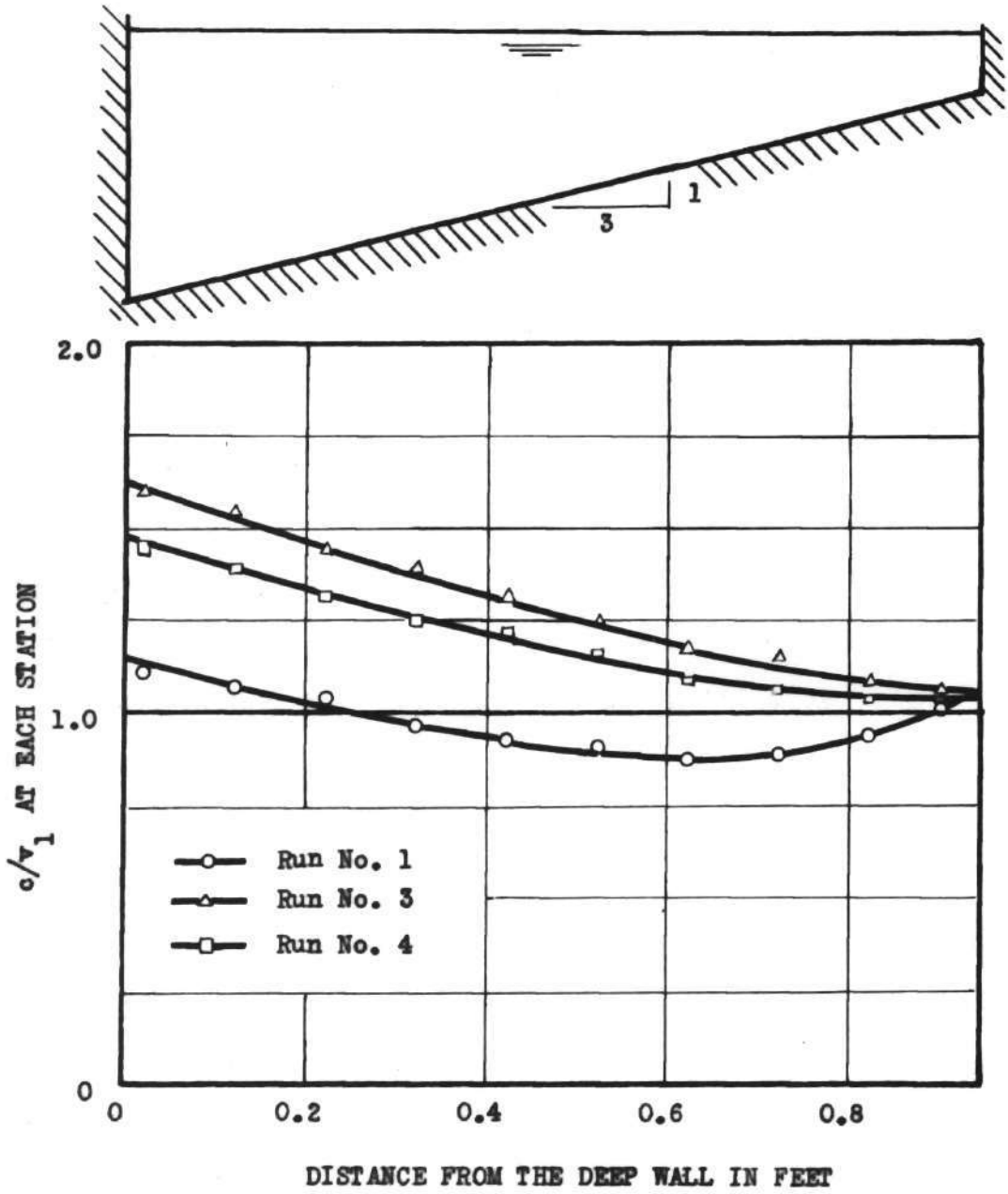

Fig. 13 Variation in the Ratio of the Celerity of a Small Gravity Wave to the Upstream Velocity in the Longitudinal Strips Across the Channel

Figs. 10 and 11, was sufficient to move the front into the position which was approximately perpendicular to the direction of flow. The equation for the celerity of a finite gravity wave with a nonbreaking surface was used in the ratio of the wave celerity over the velocity for Runs No. 3 and 4.

In Run No. 1, the ratio of the celerity of the gravity wave to the velocity in the upstream strip had to be expressed in two different forms. The same equation that was used for Runs No. 3 and 4 was used for Run No. 1 where the water surface profile for Run No. 1 was similar to the water surface profile obtained in Runs No. 3 and 4. The equation for the celerity of a finite gravity with breaks in the surface was used in the ratio of c/v_1 for the shallow part of the cross section. The values of the c/v_1 ratio in the deep part of the cross section were less than those obtained for Runs No. 3 and 4, but the ratio indicated that the wave front had the same general appearance as the front in Runs No. 3 and 4. The indicated wave front on the shallow side was different as can be seen in Fig. 13. The value of the c/v_1 ratio increased from the deep part of the channel cross section where the fully developed hydraulic jump started toward the shallow side of the cross section. The increase in the c/v_1 ratio indicated that there was a tendency for the wave front to change from the downstream direction to an upstream direction. As the c/v_1 ratio was greater than one in the longitudinal strip next to the wall, the tendency of the wave front in this section of the channel was to move upstream. The transfer of momentum for Run No. 1 as seen in Fig. 12, shows that there was a transfer of momentum through both parts of the wave front that were tending to move upstream.

There was a transfer of fluid laterally from the deep side as well as momentum in all runs, as can be seen in Figs. 14, 15, and 16. Runs No. 3 and 4 had only a small amount of fluid transferred as shown in Figs. 15 and 16. As β was not greatly changed between the upstream and downstream sections, the transfer of momentum was effected by an increase in depth with the resulting decrease in the velocity. The figures were plotted from the calculated rates of flow in each strip, and as the total downstream rates of flow were less by four and ten per cent than the upstream rates of flow, the final adjustment of the flows would indicate more transfer of fluid than was shown. Time-weight measurements of the rate of flow over the time used to complete a run varied by as much as three per cent; therefore, the calculated rates of flow were adjusted accordingly to satisfy the momentum calculations.

The Froude number varied across the channel as indicated by the theory. The Froude number for each run and each preset station is plotted in Fig. 17. In Run No. 1, the Froude number was above one for all of the stations and the mean Froude number was 1.33. Runs No. 3 and 4 had Froude numbers greater than one and less than one existing in the same cross section. The mean Froude number for Run No. 3 was 0.87 and for Run No. 4 was 0.92. While the calculation of the Froude number in the longitudinal strips indicate that there is rapid flow in the same channel with tranquil flow, the standing wave shows that such is not the actual case. The transfer of momentum and fluid was large enough to produce the standing wave across the channel; therefore, the transfer of momentum and fluid prevented the tranquil flow and rapid flow from existing in the same channel at the same time.

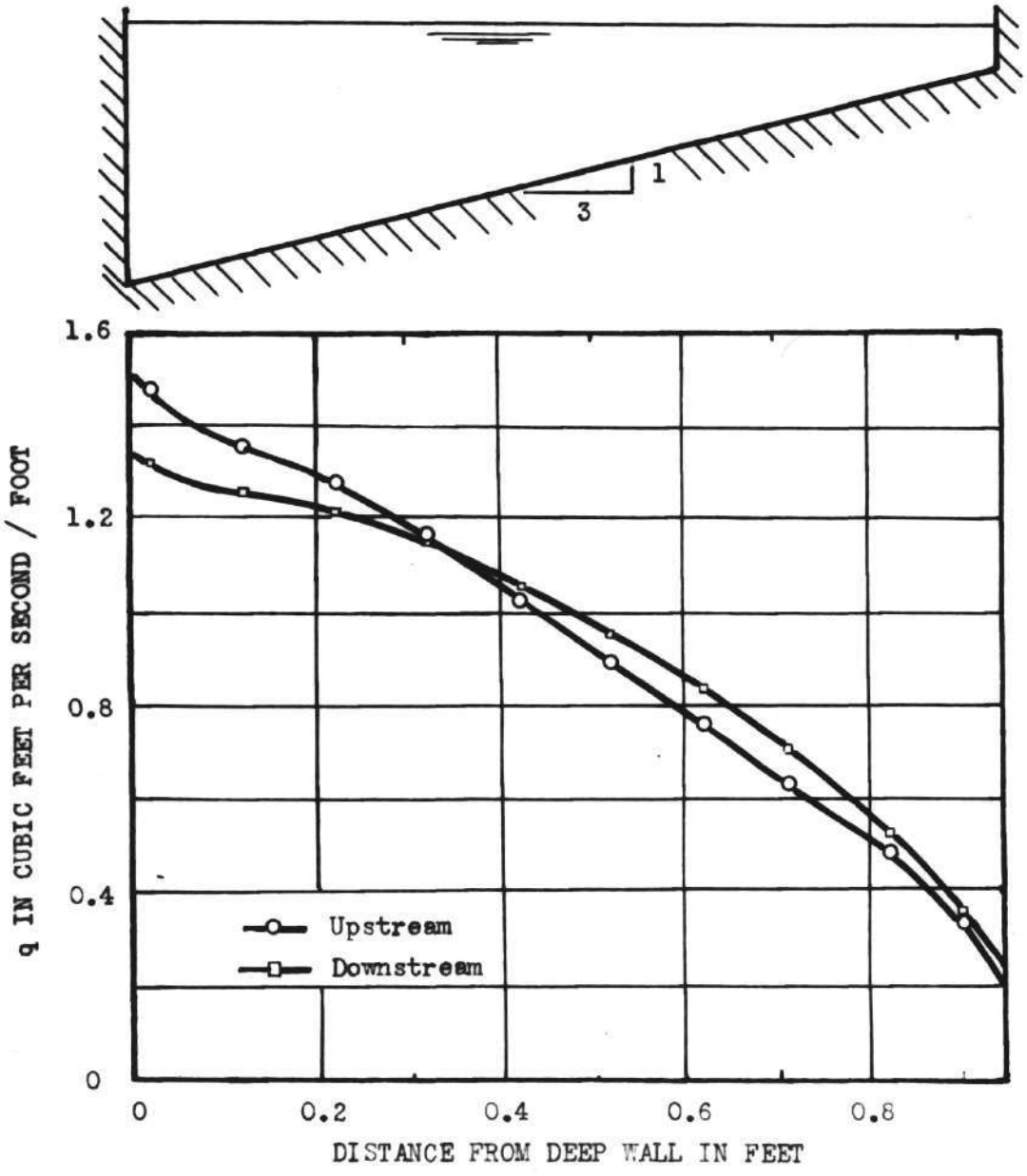

Fig. 14 Variation of Upstream and Downstream Unit Rates of Flow Across the Channel for Run No. 1

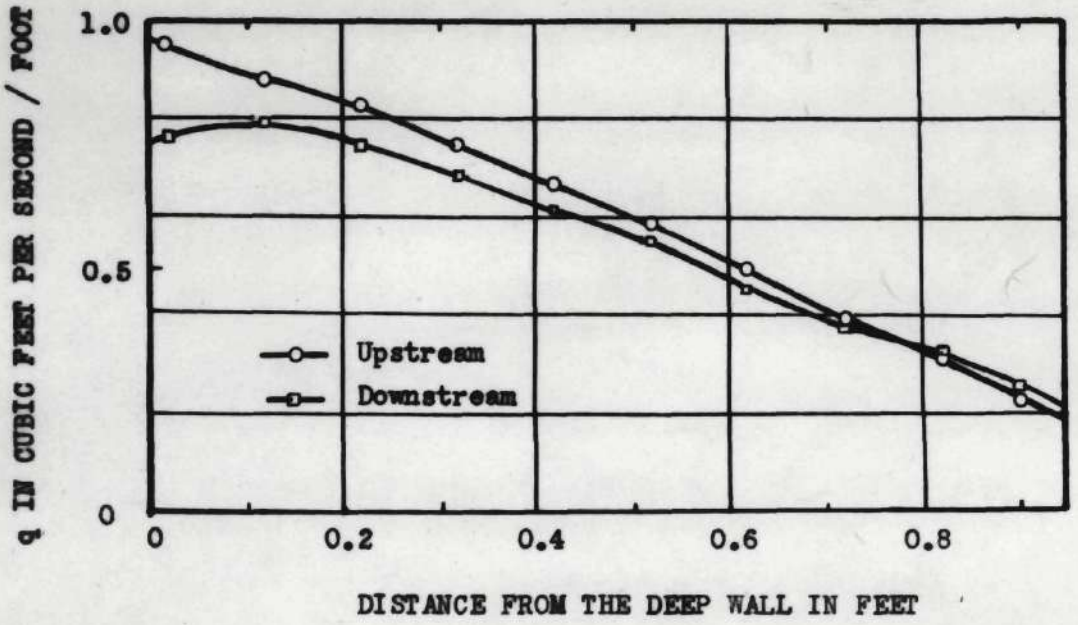

Fig. 15 Variation of Upstream and Downstream Unit Rates of Flow Across the Channel for Run No. 3

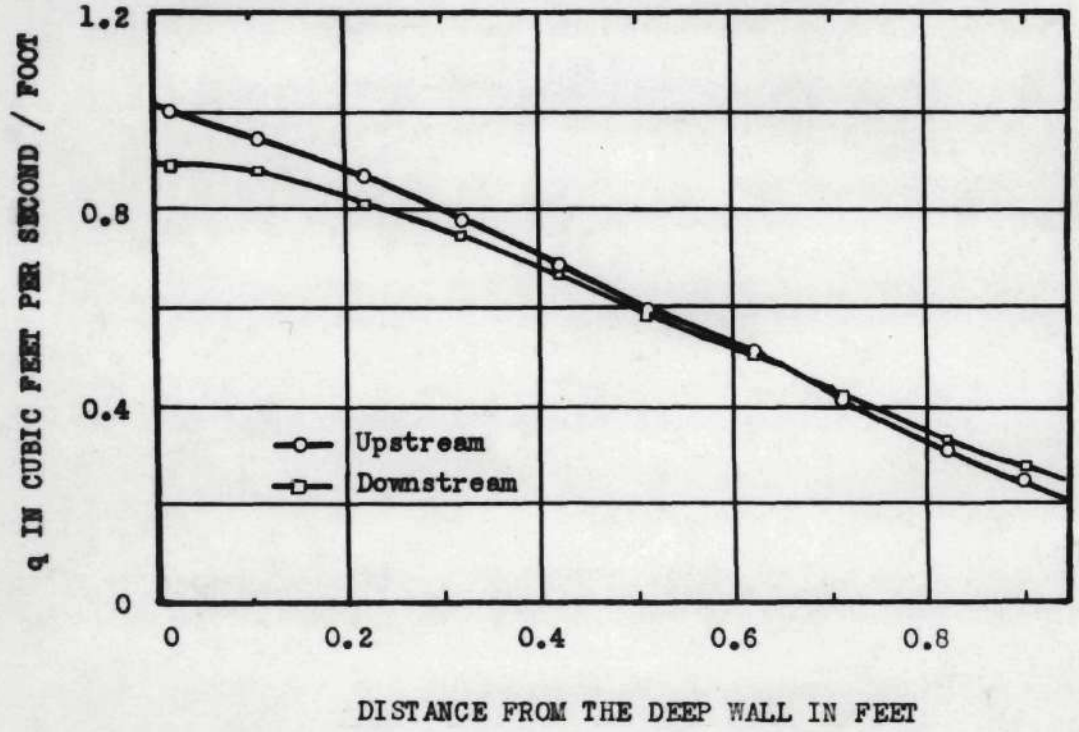

Fig. 16 Variation of Upstream and Downstream Unit Rates of Flow Across the Channel for Run No. 4

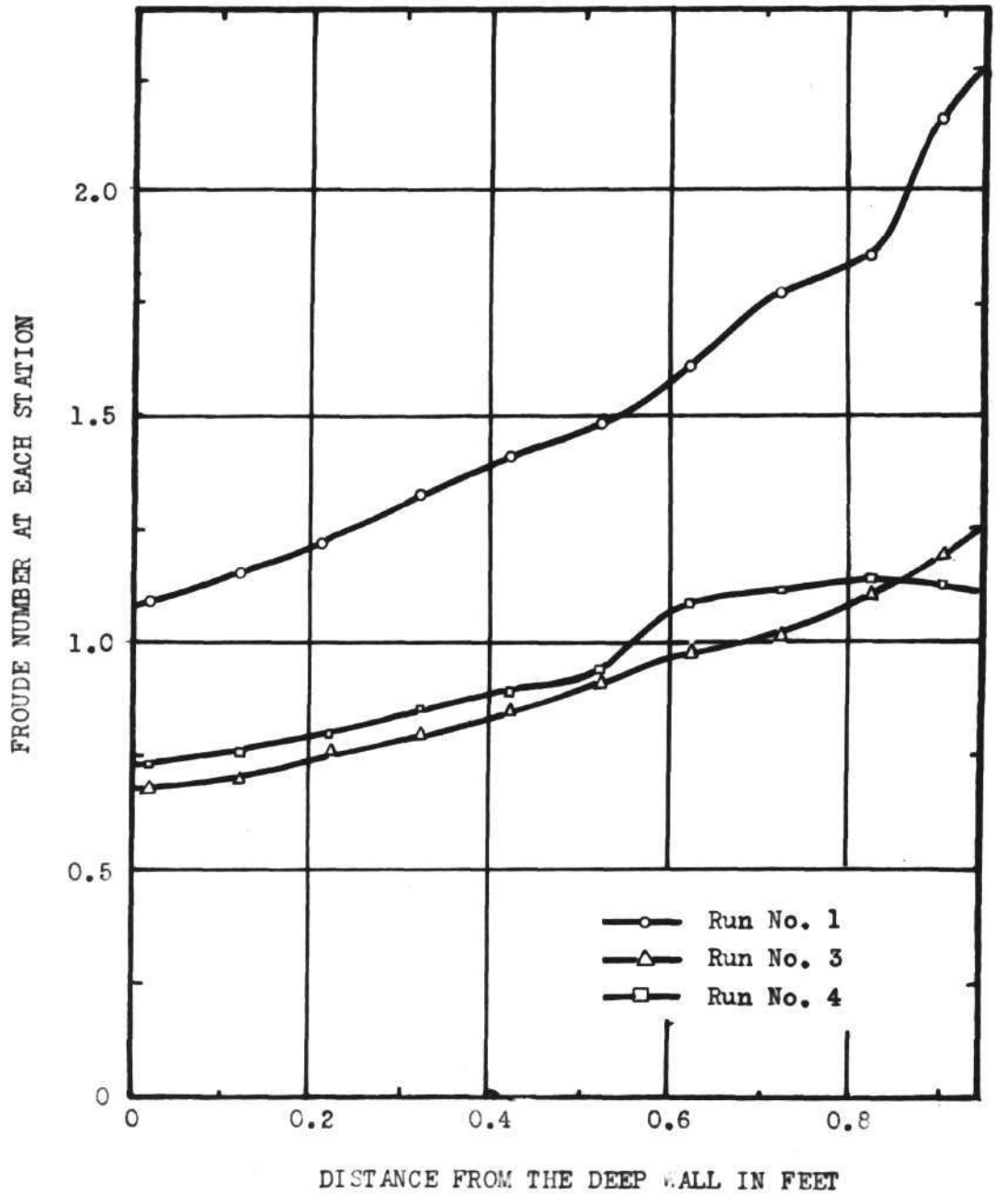

Fig. 17 Variation of the Froude Number with the Variation of the Depth Across the Channel Upstream

CHAPTER VI

CONCLUSIONS

The critical depth as calculated by the specific energy equation, the pressure plus momentum equation, and the gravity wave analysis was less than the actual critical depth obtained in the open channel used in this investigation. As a standing wave of finite amplitude was obtained in all runs, the upstream depth in all runs was less than the critical depth. As a gravity wave of finite amplitude will move upstream at the critical depth, the critical depth was greater than the upstream depth found in all of the runs. The mean velocity in all runs was greater than the velocity required for the critical condition.

The longitudinal strip analysis revealed that there is a transfer of momentum and fluid laterally across the channel. This transfer is caused by the movement of momentum along the wave front as the wave front tries to form at an oblique angle to the direction of flow. This lateral transfer of momentum and fluid showed why the equation for the gravity wave analysis did not give the correct wave front. Even though the Froude number in the longitudinal strips at the upstream cross section were less than and greater than one, the lateral transfer of momentum and fluid make it impossible to obtain rapid and tranquil flow in a nonrectangular channel at the same time. The lateral transfer of momentum and fluid showed that the total section must be used in the analysis of flow in an open channel with a nonrectangular cross section.

In the calculation of the critical depth by the specific energy equation, an increase in the kinetic energy correction factor, α, causes an increase of the critical depth. In the calculation of the critical depth by the pressure plus momentum equation, an increase in the momentum correction factor, β, caused an increase in the critical depth. In both cases, the effects of α and β were enough to justify their calculation in any further study of the situation.

In the analysis of flow in an open channel by the pressure plus momentum equation, the pressure forces of the actual section must be used if an equivalent rectangular section is used.

Even though there was no conclusion reached in this investigation as to what is the correct critical depth, several very interesting facts were determined which will be of help in future studies of this problem.

CHAPTER VII

RECOMMENDATIONS

A method for determination of the actual critical depth in an open channel with a nonrectangular cross section would be of great benefit to hydraulic engineers. In view of this fact, continued study of this problem would be well worth-while.

In any further investigation of this problem, several points on the pressure plus momentum curve and specific energy curve should be obtained which are closer to the actual critical point than was obtained in this study. The desired results could be obtained by the flow condition where the gravity wave is as small as can possibly be obtained. This could be done by decreasing the amount of roughness downstream and, therefore, decreasing the normal depth of flow, y_2, downstream, or by decreasing the rate of flow slightly.

In future work with the equipment used for this study, it is recommended that some modification be made to obtain a more steady rate of flow. An addition of suction lines along the deep side of the inlet would improve the velocity distribution in that region.

APPENDIX

GLOSSARY OF ABBREVIATIONS

y_1	-	depth upstream in the longitudinal strip
y_2	-	depth downstream in the longitudinal strip
y_o	-	maximum depth in the cross section
y_{ave}	-	average depth in the cross section
y_{M_c}	-	mean depth at critical velocity
F strip	-	Froude number in the longitudinal strip
F section	-	Froude number of the whole cross section
F_1	-	Froude number upstream in the longitudinal strip
q	-	rate of flow for each station in cfs/ft.
Q	-	total rate of flow
1/m	-	slope of the channel bottom laterally across the channel
ρ	-	mass density
α	-	kinetic energy correction factor
β	-	momentum correction factor
γ	-	unit weight
M_o	-	pressure plus momentum for the bulk section
H_o	-	specific energy for the bulk section
V_1	-	average velocity in upstream cross section
V_2	-	average velocity in downstream cross section
v_1	-	average velocity in upstream longitudinal strip section
v_2	-	average velocity in downstream longitudinal strip section
c	-	celerity of a finite gravity wave

EQUATIONS USED

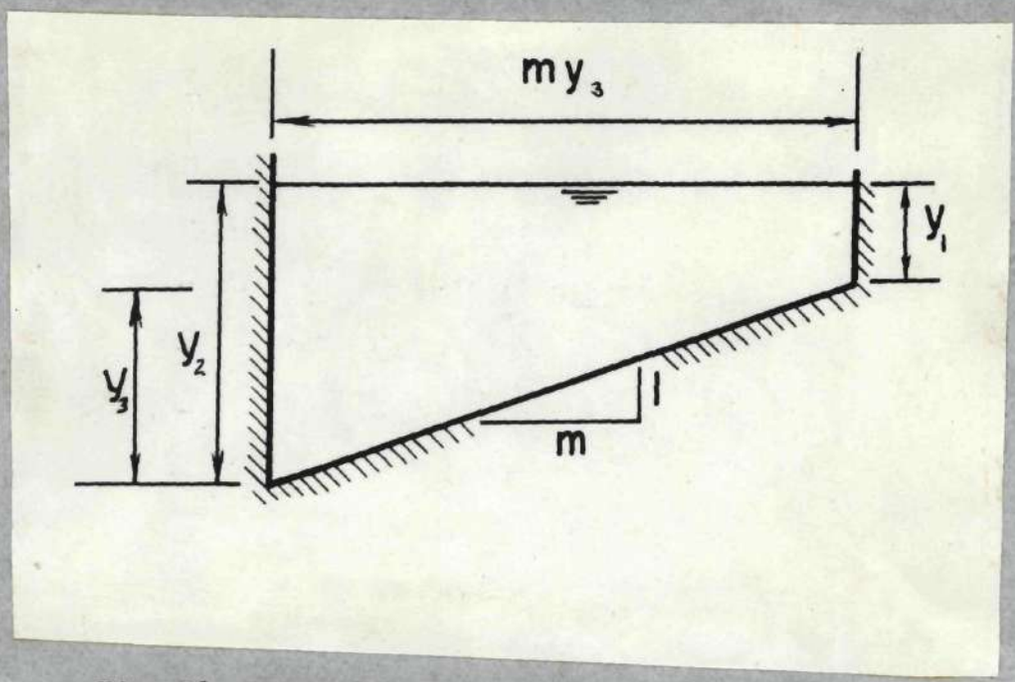

Fig. 18 ACTUAL CROSS SECTION OF THE CHANNEL USED IN THE INVESTIGATION

Pressure plus momentum equation for the actual cross section used

$$\gamma M_o = P + M$$

$$\gamma M_o = \gamma m y_3 \left[\frac{y_1^2}{2} + \frac{m y_1 y_3}{6} + \frac{m^2 y_3^2}{54} \right] + \frac{\rho \beta Q^2}{m y_3 \left(y_1 + \frac{m y_3}{6} \right)}$$

Pressure plus momentum equation for the dimensionless plot.

$$\frac{M_o}{\gamma y_{M_c}^3} = \frac{m y_3}{y_{M_c}^3} \left[\frac{y_1^2}{2} + \frac{m y_1 y_3}{6} + \frac{m^2 y_3^2}{54} \right] + \frac{\beta m y_3}{\left(y_1 + \frac{m y_3}{6} \right) g}$$

Pressure plus momentum equation between the upstream and downstream cross sections.

$$\Sigma F_D - \Sigma F_U - \text{Wt. component} = \rho Q(\beta_1 V_1 - \beta_2 V_2)$$

$$\left[(y_1 my_3)(y_1/2) + \frac{(my_3)}{2}(y_3)(y_1 + \frac{my_3}{3})\right]_{Dn.} - \left[y_1(my_3)\frac{(y_1)}{2} + \frac{(y_3)}{2}(my_3)(y_1 + \frac{my_3}{3})\right]_{up.} - (\text{Wt. of Fluid Between Upstream and Downstream})(\text{slope}) = \rho Q(\beta_1 V_1 - \beta_2 V_2)$$

Momentum deficiency or surplus in each longitudinal strip

$$\frac{\text{Momentum Difference}}{\text{Pressure Difference}} = \frac{\rho \int v_1^2 dy - \rho \int v_2^2 dy}{\gamma \frac{y_2^2}{2} - \gamma \frac{y_1^2}{2}}$$

Trapezoidal Rule

$$\text{Area} = (1/2\, y_o + y_1 + y_2 + \ldots\ldots + y_{n-1} + 1/2 y_n)\Delta X$$

Specific energy equation for the total cross section

$$H_o = \frac{2}{2y_1 + y_3}\left[\frac{\alpha V^2}{2g}(y_1 + \frac{y_3}{2}) + (y_1^2 + 2y_1 y_3 + 2/3\, y_3^2)\right]$$

Ratio of the celerity of a gravity wave with no breaks in the surface to the velocity in the upstream section of the longitudinal strip.

$$\frac{c}{v_1} = \frac{1}{\sqrt{F_1}}\left(1 + \frac{3}{2}\frac{y}{y_1}\right)^{1/2}$$

Ratio of the celerity of a gravity wave with breaks in the surface (through a hydraulic jump) to the velocity in the upstream section of the longitudinal strip.

$$\frac{c}{v_1} = \frac{1}{\sqrt{F_1}}\left[1/2\,\frac{y_2}{y_1}\left(\frac{y_2}{y_1} + 1\right)\right]^{1/2}$$

BIBLIOGRAPHY

BIBLIOGRAPHY

LITERATURE CITED

1. Lane, E. W. and Kindsvater, C. E. "Hydraulic Jump in Enclosed Conduits" Engineering News-Record, Vol. 121, Dec. 29, 1938, pp. 815-17.

2. Posey, C. J. and Hsing, P. S. "Hydraulic Jump in Trapezoidal Channels" Engineering News-Record, Vol. 121, Dec. 22, 1938, pp. 797-8.

3. DeLapp, W. "Calculating the Critical Depth in Trapezoidal Channels" Engineering News-Record, Vol. 141, Dec. 23, 1948, p. 82.

4. Kirpich, P. Z. "Dimensionless Constants for Hydraulic Elements of Open Channel Cross-Sections" Civil Engineering, Vol. 18, Oct. 1948, p. 47.

5. Streeter, V. L. Fluid Mechanics, First Edition, New York, McGraw-Hill Book Company, 1951, p. 262.

6. Vennard, J. K. Elementary Fluid Mechanics, Second Edition, New York, John Wiley and Sons, Inc. 1950, p. 212.

7. Streeter Op. Cit. p. 262.

8. Vennard Op. Cit. p. 212.

9. Rouse, Hunter, Editor, Engineering Hydraulics, New York, John Wiley and Sons, Inc., 1950, p. 602.

10. Posey and Hsing, Op. Cit.

11. Rouse, Op. Cit. p. 73.

12. Rouse, Op. Cit. p. 508.

OTHER REFERENCES

13. Bakhmeteff, B. A. Hydraulics of Open Channels, New York, McGraw-Hill Company, 1932.

14. Goldstein, S., Editor, Modern Developments in Fluid Dynamics, Vol. II Oxford, England, Clarendon Press, 1938, p. 529.

15. Jaeger, C. "Steady Flow in Open Channels: Problem of Boussinesq" Institution of Civil Engineers of London Journal, Vol. 29, Feb. 1948, pp. 338-49.

16. Prandtl, L. and Tietjens, O. G. Applied Hydro and Aero Mechanics New York, McGraw-Hill Book Company, Inc., 1934, p. 294.

17. Rouse, Hunter Elementary Mechanics of Fluids New York, John Wiley and Sons, Inc., 1946.

18. Rouse, Hunter Fluid Mechanics for Hydraulic Engineers First Edition, New York, McGraw Hill Book Company, 1938, p. 369.